Plasmonic Metalens for Narrowband Dual-Focus Imaging

Calum Williams,[*,†,§] Yunuen Montelongo,[‡,¶,§] and Timothy D. Wilkinson[†]

†*Centre of Molecular Materials for Photonics and Electronics, Electrical Engineering Division, Department of Engineering, University of Cambridge, 9 JJ Thomson Avenue, Cambridge CB3 0FA, United Kingdom*

‡*Department of Chemistry, Imperial College London, Exhibition Road, South Kensington, London SW7 2AZ, United Kingdom*

¶*Universidad De La Salle Bajío, León, 37150, Mexico*

§*equal contribution*

E-mail: cw507@cam.ac.uk

Abstract

We report a new type of metalens with the capability to selectively focus narrowband light at different focal planes depending on polarization. Two zone planes with two different focal lengths are spatially multiplexed and encoded, in the sub-wavelength regime with arrays of orthogonal silver nanostructures, which are designed to exhibit strong wavelength- and polarization-dependent scattering profiles. Using this principle, we experimentally demonstrate imaging under white light illumination with independent focal planes for each polarization at the narrow band resonant wavelength. Furthermore, each focal plane can be dynamically controlled with an output polarizer. In contrast to conventional refractive and diffractive optical elements, functional metalenses allow additional control over wavelength and polarization properties of light for a wide range of applications.

Introduction

Diffractive optical elements (DOEs) are versatile components used to generate arbitrary complex wavefronts.[1,2] DOEs have microstructured surfaces—which can be fabricated with monolithic techniques, as opposed to conventional mechanical lens grinding—and through diffraction, can replicate the performance of their refractive counterparts in a highly reduced form factor. DOEs provide optical functionality beyond that which can be achieved with a single refractive element. This includes aberration correction, beam shaping and multiplexing multiple optical elements—such as multi-focus lensing—in single elements.[1,2] As a result, through the hybridization with refractive optics, or by substitution, DOEs offer a broad optical design toolbox for a plethora of applications in reduced form factors.[2]

With the continual shrinking of optical systems—from the macro-to-micro optical realms[2]—the inevitable form factor reduction of DOEs leads to two important disadvantages, which arise from their diffractive nature. The first, is a result of the relatively large dimensions necessary to observe diffraction. According to the Geometrical Theory of Diffraction (GTD),[3] to observe a considerable wave perturbation, features with dimensions $\geq \lambda/2$ are necessary. Although the GTD predicts arbitrary numerical apertures (NA), the physical dimension to produce diffraction imposes a physical constraint.[4] The second disadvantage arises from the lack of functionality of the diffractive structures, which are restricted in order to create constructive interference at the focal point. In recent years, the advent of nanophotonic devices—based on the control of the optical wavefront over sub-wavelength length scales—has opened up a new class of planar optical element: the metasurface.[5–9] Optical metasurfaces present a route toward enhancing the DOE further, whereby the control of highly localized optical fields across the element can impart additional optical functionality such as amplitude, wavelength, polarization and phase modulation.[5,6,9,10]

The unique light-matter interaction with nanostructured metals leads to the excitation of localized surface plasmon polaritons, resulting in highly pronounced and tunable scattering cross-sections.[5,11–13] With noble metals, this behavior occurs at visible wavelengths[12,14] and

through tailored arrays of such sub-wavelength scatterers (metasurfaces) arbitrary control of the optical wavefront is possible. A myriad of metasurface devices have been previously demonstrated, including beam shapers, polarizers and lenses, referred to as metalenses.[9,15–18] Previous work, either metallic(plasmon-based) or, more recently, dielectric-based metasurfaces, generally aim to mimic functionality of conventional broadband optical elements but through ultrathin form factors, termed *flat optics*.[8,9,19–21] However, utilization of the unique optical properties of metallic-or-dielectric-based nanoscale resonators[9]—such as strong wavelength or polarization dependence—in combination with well established DOEs, for more elaborate design schemes, has great potential.

In this work, we introduce a plasmonic-enhanced metalens which has the ability to selectively focus light of a certain wavelength, to two different focal planes, depending on polarization state. Through tailored arrays of ultrathin plasmonic nanostructures on silicon, we experimentally demonstrate two types of reflective metalens: a Fresnel zone plate and a photon sieve; with dual-focusing capability, dependent on polarization. For each type, two different focal length lenses are encoded with orthogonal anisotropic silver nanostructures, which are designed to exhibit specific scattering spectra (reflection response). The resultant nanostructured optical element controls two orthogonal polarizations at the resonant wavelength, reconstructing the respective polarizations at two independent focal planes. The advantage of this type of lens is that two focal points can be activated independently and on-axis. There are a range of applications in which components exhibiting narrowband wavelength and polarization dependent optical modulation in ultrathin form factors is highly desirable including optical disc technologies, laser-based projector systems and head mounted displays.[1,2]

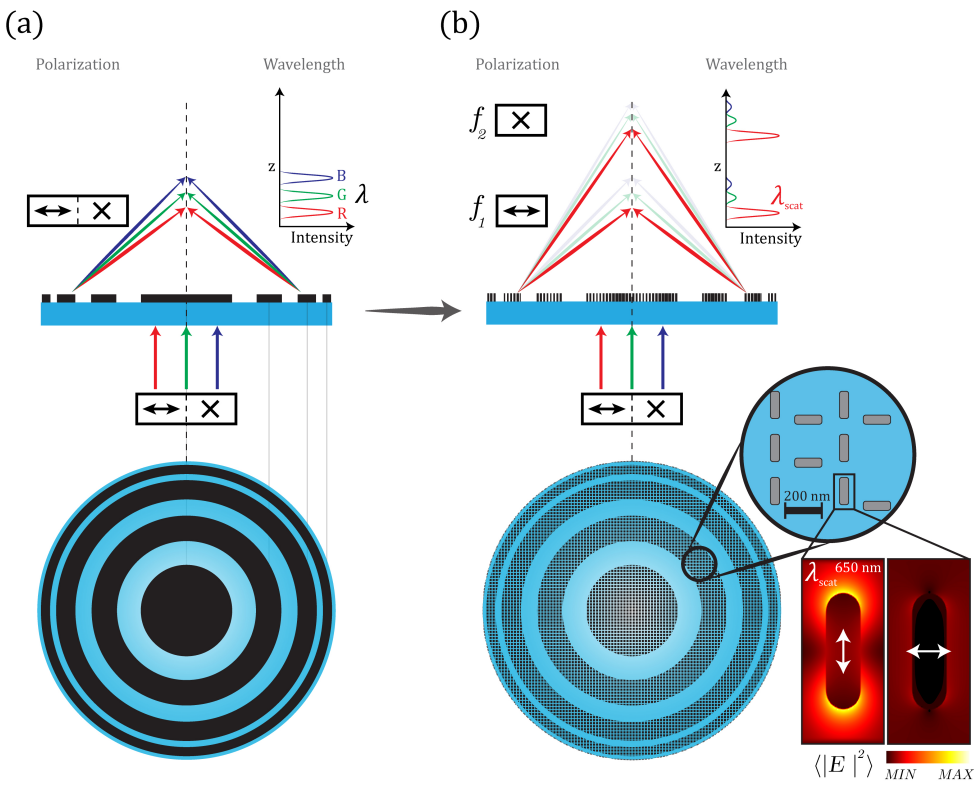

Figure 1: Concept introduction: An illustration of the difference between conventional binary-diffractive lens (zone plate) and proposed plasmonic-enhanced lens for orthogonal linearly polarized input. (a) Binary transmittance regions composed of a thin opaque material, such as chromium. (b) Plasmonic-enhanced flat-lens (metalens), whereby the lens in (a) is now composed of sub-wavelength scattering elements (metallic nanostructures) providing wavelength and polarization dependent scattering through polarization dependent localized surface resonance (LSPR)—shown through FDTD simulations of a silver anisotropic nanostructure.[22] Multiplexing two focal length lenses with such structures leads to orthogonal polarizations being focused at two positions at the resonant wavelength—determined by the LSPR.

Diffractive metalens

Operating principles

A diffractive lens consists of concentric micro-structured reliefs in which the principle of diffraction, rather than refraction, is used to focus the light. Two types of structures have shown the capabilities to focus light at a given distance from the diffraction plane: Fresnel Zone Plates (FZP) and Photon Sieves (PS). In the case of a FZP, the output corresponds to the constructive interference at the focal point. The diffraction is produced by concentric

consecutive rings at the FZP plane. Each ring has a radius given by,[23]

$$r_n^2 = n\lambda f + \frac{n^2\lambda^2}{4}. \tag{1}$$

The focal length of the FZP is given by f, n is an integer representing the n^{th} ring boundary from the FZP centre, and λ is the illumination wavelength. Hence a binary FZP uses symmetrical alternating rings (zones), whereby diffraction from the transparent regions interferes, focusing the transmitted light.[1,2] Moreover, ZPs can be simplified with a binary transmittance function—shown in Fig. 1(a)—offering reduced fabrication complexity yet still maintaining a reasonable focusing efficiency. An extension to the FZP is the photon sieve (PS), which is capable of focusing light, through a pinhole modification to the alternating FZP circular rings.[24,25] In practical terms, the transmission regions are replaced with circular apertures located at the same radial distance as the FZP rings. The maximum diameter of a circular aperture, for full packing, is given by:

$$w_n = r_{n+2} - r_n. \tag{2}$$

The PS has been shown to improve FZP focusing performance and is relatively easier to fabricate than a conventional FZP.[24,25] Nevertheless, in either case, the zones / holes offer no other functionality other than applying a spatially varying broadband transmittance function to the incident light. By nanostructuring the ZPs, the unique nanoscale light-matter interaction can be utilized to impart customizable scattering profiles over sub-wavelength dimensions on the lens; specifically, strong wavelength and polarization dependency. This idea is represented by the plasmonic-enhanced metalens in Fig. 1(b).

Through appropriate design and material choice, the plasmonic resonance—and subsequent scattering spectra—of metallic nanostructures can be tuned.[11] With arrays of tailored scatterers, 'surfaces' can be engineered which exhibit a specific spectral and polarization response detectable in the far-field.[5,7,13,13,26,27] Fig. 2 illustrates the underpinnings of the pro-

posed metalens operation. The length of the anisotropic metallic nanostructure determines the wavelength of operation (scattering cross-section), through localized surface plasmon resonance (LSPR),[12] and its aspect ratio (anisotropy) determines polarization selectivity (spectrally dependent extinction ratio). Fig. 2(a) shows finite-difference time-domain (FDTD) simulations[22] of the normalized scattering cross-sections for varying length anisotropic nanos-

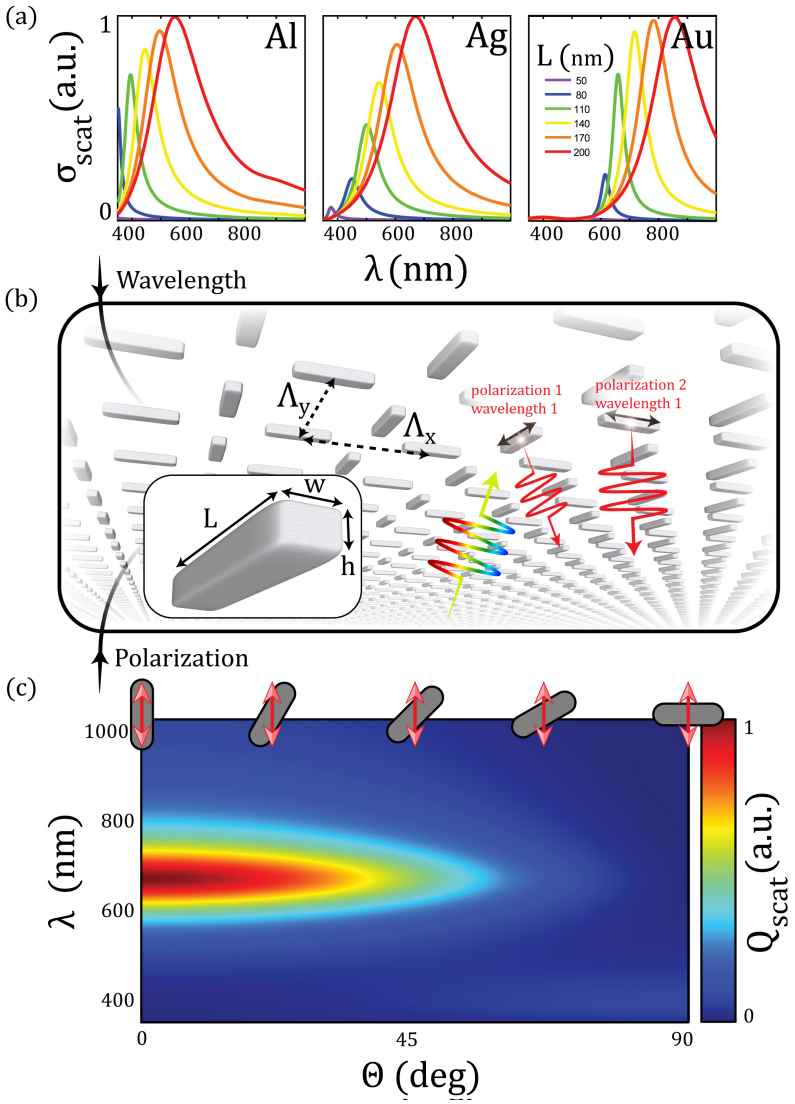

Figure 2: (a) Normalized scattering cross sections from FDTD simulations[22] for a range of anisotropic (50 nm X 50 nm X L) metallic (Al, Ag, Au) elements for the co-polarization condition. (b) Arrays of orthogonal anisotropic Ag elements yields a surface with wavelength and polarization output properties. (c) Simulated reflection response map of the polarization dependent response of an Ag element ((50 nm X 50 nm X 160 nm) designed to operate in the red (650 nm) part of the visible spectrum, under varying in-plane rotations.

tructures composed of three different metals (Al / Ag / Au). Ag is chosen as the material of choice for this work, as a trade off between narrow-band optical response in the visible and length required to achieve this output. Specifically, in relation to nanofabrication tolerances, the reproducible resolution of the system means that aspect ratios can be optimized for larger structures, yet a larger structure inevitably induce second-order LSPRs (such as for Al).[11] Operation in the red (∼650 nm) part of the spectrum is selected for this study. Next, the length of nanostructure identified – Fig. 2(c) shows the simulated scattering response, of an anisotropic Ag nanostructure ((50 nm x 50 nm x 160 nm) for different polarization conditions, at a fixed wavelength of 650 nm. Akin to linear polarizers, this response is indicative of a spectrally-dependent Malus law,[28] whereby initial intensity is the co-polarization state response (LSPR) of the anisotropic structure.

Fig. 3(a–b) illustrates the metalens design process. The spatially varying binary transmittance function for each zone plate is calculated,[1,2,24] spatially discretized and sampled with the anisotropic elements.[27,28] For overlapping zone plates, the respective structures are orthogonal and separated by ∼≥100 nm to avoid cross-talk.[13] The ZPs are spatially multiplexed, and transverse nanostructures are used as the fundamental scattering element (L = 160 nm) in a 390 nm unit cell, which are designed to give optimal red reflection λ ∼650 nm. The two lens types are ∼156 μm in diameter, with designed independent focal lengths of 125 μm and 250 μm. The fabricated lenses are shown under scanning electron microscope (SEM) in Fig. 3(c–d) at varying magnifications, with indications of varying polarization dependent regions highlighted. A ZP of this nature—composed of functional optical diffractive units (plasmonic scatterers)—has the potential to selectively focus light according to polarization and wavelength. Moreover, spatially multiplexing different ZPs (with varying focal lengths) allows a single ultrathin layer to exhibit multiple focal lengths. It is straightforward to scale these designs for larger focal lengths and operating wavelengths.

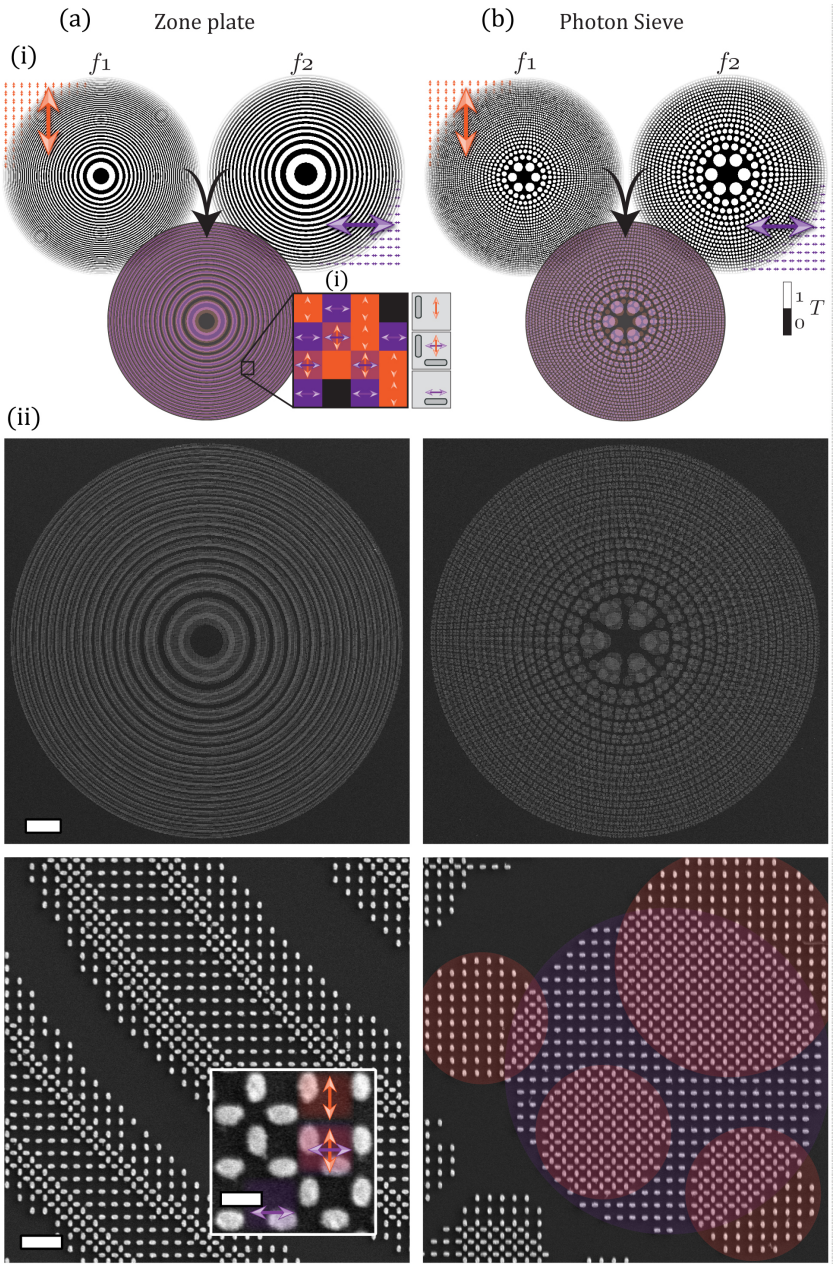

Figure 3: Dual-focus metalens design process: Two different focal length, binary amplitude only FZPs (a) and PSs (b) are spatially multiplexed and encoded using orthogonal polarization states i.e. anisotropic plasmonic nanostructures (i). The fabricated lenses, comprising arrays of 50 nm thick Ag nanostructures, based on the design process above, are shown in (ii) under SEM at varying magnifications. The bottom right magnification is used to indicate (through color highlights) the two lenses spatially multiplexed on one another using the orthogonal nanostructures. The scale bars are 10 μm (top), 1 μm and 200 nm respectively.

Experimental methodology

80 kV electron beam lithography (EBL) (Nanobeam Ltd., nB-1) is used for the high-resolution patterning of the nanostructures on polished Si-SiO_2(300 nm). PMMA (Polymethyl-methacrylate)

A4 950k positive tone photoresist (baked thickness $\sim$ 150 nm) is used in combination with EBL exposure conditions: Area dose 20 μC cm^{-2} and current 5 nAs^{-1}. Resist development is carried out in a solution of MIBK (Methyl-isobutyl-ketone): IPA (Isopropyl alcohol) (1:3), for $\sim$10s. Deposition of Ag(50 nm) is performed using a thermal evaporator at a base pressure $\lesssim 1\times10^{-6}$mbar. Resist lift-off is carried out in N-Methyl-2-pyrrolidone (NMP), at an elevated temperature of 60°C for 4 hours, followed by fresh NMP sonication and IPA rinse. White light optical characterization is performed using an Olympus BX-51 polarizing optical microscope, with halogen bulb light-source, optically attached to an Ocean Optics HR2000+ spectrometer and image sensor on the output arm. A rotating achromatic linear polarizer (analyzer) controls the polarization state reaching the sensor and an aperture stop is used to control the angular distribution of light illuminating the lenses. Alternatively, for single wavelength operation, a red (650 nm) laser diode (5 mW) is used in conjunction with a custom optical cage-mounted set-up, which includes a XYZ translation stage and image sensor. Further details on the optical characterization are included in the supplementary information (SI). For surface quality inspection, a Carl Zeiss SEM operating at 1–5 keV is used.

Results and Discussion

Principle demonstration with laser illumination

In order to test the capabilities of the metalens, we simulated the field produced by the different metalenses and then compared with the intensity experimentally measured along the propagation axis. We reduced the complexity of the complete 3D FDTD simulation approach by considering the propagation as a result of interference from an array of spherical scatterers, or Huygens wavelets (each described by $\exp(i\mathbf{r}.\mathbf{K})$, where $\mathbf{r}$ is the position vector and $\mathbf{K}$ the wavevector). This simulation only reproduces the propagation of a single polarization, therefore each metalens consisted of two independent simulations for each polarization. Fig.

4 shows a comparison between simulated and experimental results of the two metalenses under red laser diode (650 nm) illumination.

The lenses were excited with two orthogonal polarizations and the resultant re-radiated field intensity mapped onto the propagation axis. The mapping was obtained with a microscope focusing at different focal planes; from the lens plane to 300 μm. The two focal planes are $\sim$125 μm and $\sim$250 μm for each orthogonal polarization. The apparent crosstalk shown through simulations in fact arises from further diffraction orders, and not from the unwanted polarization. Experimental measurements also show additional cross-talk, which may arise from fabrication error (reduction of nanostructure anisotropy, hence extinction ratio reduction). Intensity cross-sections through the radial axis are shown in Fig. 4(a–b, iii). Relatively narrow ($\sim 3\ \mu m$) FWHMs and large signal-to-noise of the focal point intensity at both polarizations can be observed.

White light illumination

Similarly, we studied the performance of both types of metalenseses with a white light source. Fig. 5 shows the experimental measurements under white light illumination (unpolarized incoherent input) using optical microscopy, for the FZP and PS metalenses. Fig. 5(b) shows the optical reflection spectra of the lens array, with collection spot (from multi-mode fiber) located at the respective focal spots. The optical response peaks at the target red wavelength (650 nm) for both planes, but the 2nd exhibits reduced peak intensity. With the microscope image plane aligned to the lens plane, varying the analyzer (0, 45, 90 °) reveals an in-plane color change—shown with both FZP (c) and PS (d). For the two focal planes, 2D intensity maps at the different analyzer states are shown in Fig. 5(c–d, ii). Because the spectra in (b) peaks in the red part of the spectrum, the red-channel pixel data is extracted for this analysis. Polarization dependent focusing at the two different focal planes is observed, yet there is clear cross-talk between the two orthogonal polarization states. Even though the focusing intensity of the unwanted polarization (at the respective focal plane) are similar

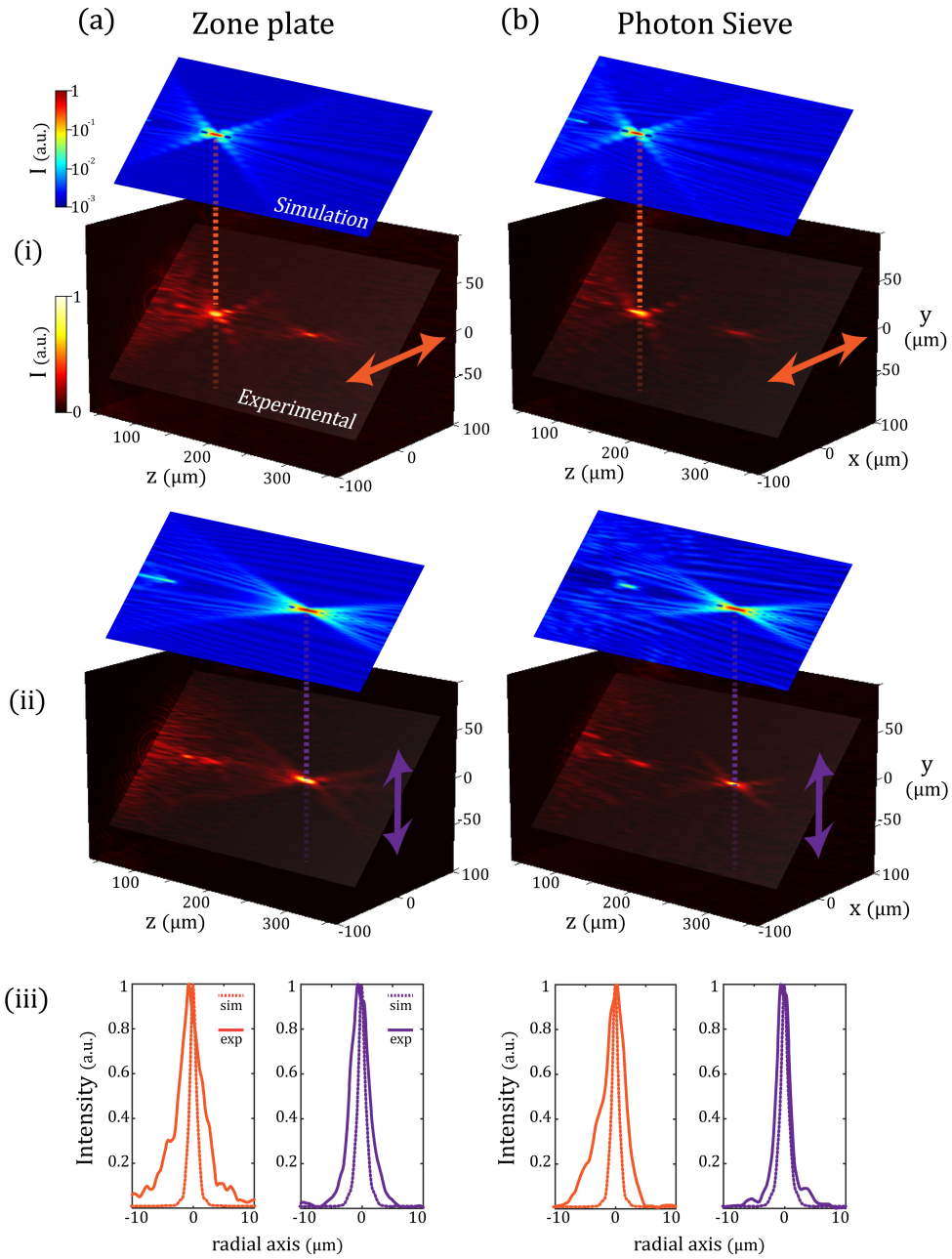

Figure 4: Lens focusing of the FZP (a) and PS (b) at the two focal planes for orthogonal polarizations shown through both simulations and experimentally. (i) Focal point 1 (125 μm) at polarization state 1. (ii) Focal point 2 (250 μm) at polarization state 2. (iii) Intensity cross-sections through the radial axis at the two focal planes for orthogonal polarizations. The lenses were excited with a laser at 650 nm with two polarizations.

between planes, the reduced intensity of designed focus means the extinction between planes is reduced. Similarly to the laser illumination in the previous section, it is difficult to distinguish whether the apparent crosstalk arises from the unwanted polarization or from

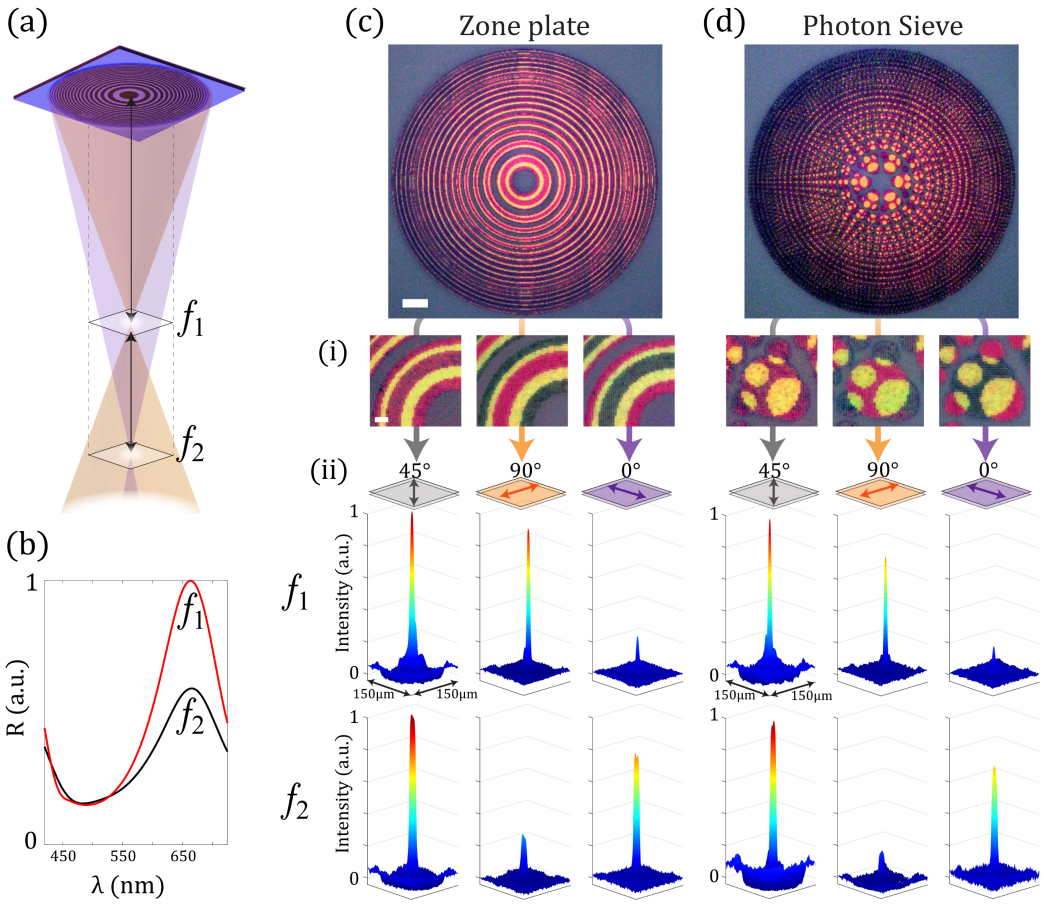

Figure 5: White light lens characterization. (a) Schematic of lens operation at the relative positions of f_1 and f_2. (b) Optical reflection spectra at the two focal planes (focal spots) for the FZP. (c) FZP and (d) PS: (i) Optical microscope images and three output polarization (analyzer) conditions (0, 45, 90 °) in reflection. (ii) are the normalized intensity profiles at the two focal planes (f_1 and f_2), for the varying analyzer states — normalized to the 45 ° analyzer state.

a different diffraction order of the excited polarization. For the respective polarizations (at each focal plane) both metalenses exhibit peak intensity-to-background intensity ratios of up to $\sim 10^2$x, and orthogonal polarization selectivity of up to ∼9x—inferred from the data extracted from Fig. 5(c–d, ii).

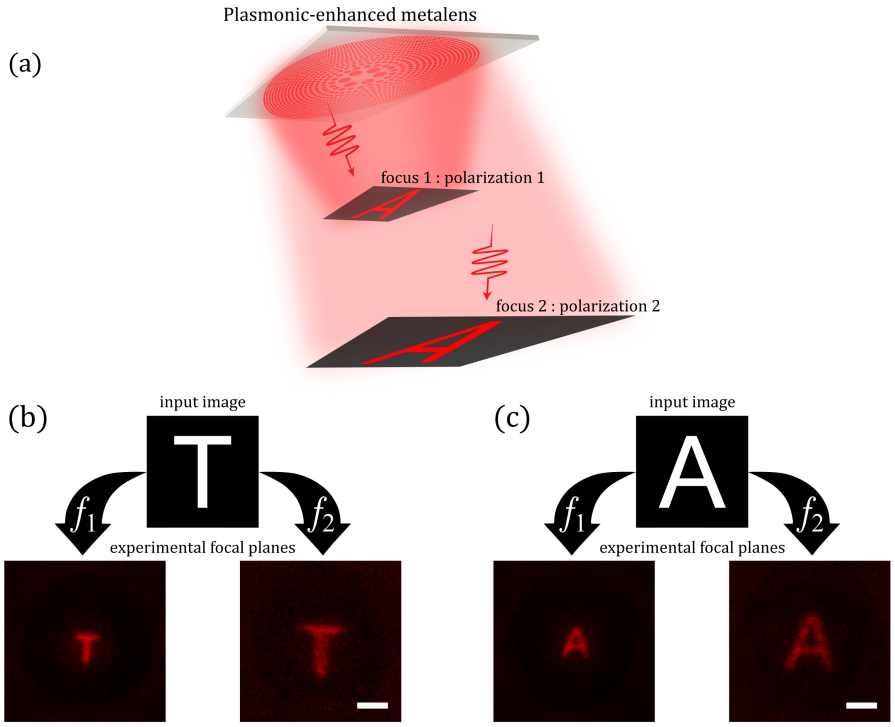

Figure 6: (a) Imaging using the plasmonic enhanced metalenses: red light is focused to two different focal planes for orthogonal polarizations. For example, for an input such as the letter "A" (broadband white light), two images are reconstructed. Experimental verification: Two binary transmittance transparencies with the letters "A" and "T" are printed and placed in the aperture stop of the microscope. FZP (b) and PS (c) metalenses are used to image the letters at the two focal planes, at orthogonal polarizations and a the target red (650 nm) wavelength. The scale bars in the images in (b–c) are 40 μm.

Imaging

Fig. 6 demonstrates white light input imaging with the metalenses. A transparency film is ink-jet printed with the letters A and T (binary transmittance) at a size of ∼2 x 2 mm each. The transparency is placed at the imaging plane for the lenses in the optical microscope (input aperture stop location). Imaging with the metalens is achieved by illuminating the transparency with unpolarized white light and a linear polarizer is added between the metalens and the focal plane to discriminate one of the orthogonal polarizations. It can be observed that the letters appear red in color, due to the scattering cross-sections of the NRs peaking at 650 nm—shown in Fig. 5(b)—hence the dominant color at the focal plane is red.

The design of the plasmonic enhanced metalenses can be tailored for any wavelength

and polarization state. A number of other DOEs (such as blazed gratings, beam splitters, beam shapers etc.) may be modified with the methodology outlined here to increase optical functionality i.e. offer specific wavelength and polarization control. Moreover, fabrication via single-step planar lithographic methods rather than a multi-step process is commercially attractive. A current limitation in the design is efficiency and narrowband operation, which can be improved through the integration of a metallic back-plane (reflection operation),[7,29] use of a dielectric-based (high-index) nanoresonator approach[9] or multi-layer thin-film arrangement.[7,26]

Conclusions

In conclusion, plasmonic-enhanced metalenses which focus light of transverse polarizations at two different focal planes have been experimentally demonstrated. Each lens is composed of two orthogonally polarized, spatially polarized zone plates or photon sieves. The macroscopic patterns are sampled with anisotropic orthogonal Ag nanostructures and then spatially multiplexed. The lens arrays are shown to operate with both laser and white light illumination, showing focusing at two focal depths with reflectance peak at the resonant wavelength, due to the tailored plasmonic resonance of the nanostructures. The lenses—under white light illumination—were used to image letters placed at the image plane and the reconstruction of each letter, at the target wavelength, for each focal plane and polarization, was observed. We envisage that these types of functional metalenses will be expanded to control other characteristics of light such as the phase and wavelength dynamically. Furthermore, lenses of this type are applicable to any wavelength regime and can be of particular interest for wavelengths whereby naturally occurring materials, exhibiting the necessary optical properties for refraction, are difficult to obtain.

Acknowledgement

The authors thank James Dolan, Catherine Fitzpatrick, George Gordon, Ammar Khan, Alexander Macfaden, Jamie Oscar Tenorio-Pearl and Girish Rughoobur for their help, fruitful discussion and support during the work.

This work was financially supported by the Engineering and Physical Sciences Research Council (EPSRC): Integrated Photonic and Electronic Systems (EP/L015455/1); Cambridge Overseas Trust and the Mexican National Council on Science and Technology (CONACyT).

References

(1) Herzig, H. P. *Micro-Optics: Elements, Systems And Applications* , 1st ed.; Taylor and Francis, 1997.

(2) Kress, B. C.; Meyrueis, P. *Applied Digital Optics*, 1st ed.; Wiley-Blackwell, 2009.

(3) B.Keller, J. Geometrical Theory of Diffraction. *Journal of the Optical Society of America* **1962**, *52*.

(4) Hessler, T.; Rossi, M.; Kunz, R. E.; Gale, M. T. Analysis and optimization of fabrication of continuous-relief diffractive optical elements. *Applied optics* **1998**, *37*, 4069–4079.

(5) Yu, N.; Capasso, F. Flat optics with designer metasurfaces. *Nature Materials* **2014**, *13*, 139–150.

(6) Kildishev, A. V.; Boltasseva, A.; Shalaev, V. M. Planar Photonics with Metasurfaces. *Science* **2013**, *339*.

(7) Kristensen, A.; Yang, J. K. W.; Bozhevolnyi, S. I.; Link, S.; Nordlander, P.; Halas, N. J.; Mortensen, N. A. Plasmonic colour generation. *Nature Reviews Materials* **2016**, *2*, 16088.

(8) Genevet, P.; Capasso, F. Holographic optical metasurfaces: a review of current progress. *Reports on Progress in Physics* **2015**, *78*, 024401.

(9) Genevet, P.; Capasso, F.; Aieta, F.; Khorasaninejad, M.; Devlin, R. Recent advances in planar optics: from plasmonic to dielectric metasurfaces. *Optica* **2017**, *4*, 139–152.

(10) Quaranta, G.; Basset, G.; Martin, O. J. F.; Gallinet, B. Color-Selective and Versatile Light Steering with up-Scalable Subwavelength Planar Optics. *ACS Photonics* **2017**, *4*, 1060–1066.

(11) Giannini, V.; Fernández-Domínguez, A. I.; Heck, S. C.; Maier, S. a. Plasmonic nanoantennas: Fundamentals and their use in controlling the radiative properties of nanoemitters. *Chemical Reviews* **2011**, *111*, 3888–3912.

(12) Maier, S. A. *Plasmonics: Fundamentals and Applications*, 1st ed.; Springer, 2007.

(13) Montelongo, Y.; Tenorio-Pearl, J. O.; Milne, W. I.; Wilkinson, T. D. Polarization Switchable Diffraction Based on Subwavelength Plasmonic Nanoantennas. *Nano Letters* **2014**, *14*, 294–298.

(14) Cai, W.; Shalaev, V. *Optical Metamaterials: Fundamentals and Applications*, 1st ed.; Springer, 2010.

(15) Aieta, F.; Genevet, P.; Kats, M. a.; Yu, N.; Blanchard, R.; Gaburro, Z.; Capasso, F. Aberration-free ultrathin flat lenses and axicons at telecom wavelengths based on plasmonic metasurfaces. *Nano Letters* **2012**, *12*, 4932–4936.

(16) Aieta, F.; Kats, M. A.; Genevet, P.; Capasso, F. Multiwavelength achromatic metasurfaces by dispersive phase compensation. *Science* **2015**, *347*, 1342–1345.

(17) Duempelmann, L.; Luu-Dinh, A.; Gallinet, B.; Novotny, L. Four-Fold Color Filter Based on Plasmonic Phase Retarder. *ACS Photonics* **2016**, *3*, 190–196.

(18) Li, Z.; Clark, A. W.; Cooper, J. M. Dual color plasmonic pixels create a polarization controlled nano color palette. *ACS Nano* **2016**, *10*, 492–498.

(19) Chen, X.; Huang, L.; Mühlenbernd, H.; Li, G.; Bai, B.; Tan, Q.; Jin, G.; Qiu, C.-W.; Zhang, S.; Zentgraf, T. Dual-polarity plasmonic metalens for visible light. *Nature communications* **2012**, *3*, 1198.

(20) Wang, W.; Guo, Z.; Li, R.; Zhang, J.; Liu, Y.; Wang, X.; Qu, S. Ultra-thin, planar, broadband, dual-polarity plasmonic metalens. *Photon. Res.* **2015**, *3*, 68–71.

(21) Li, R.; Guo, Z.; Wang, W.; Zhang, J.; Zhou, K.; Liu, J.; Qu, S.; Liu, S.; Gao, J. Arbitrary focusing lens by holographic metasurface. *Photon. Res.* **2015**, *3*, 252–255.

(22) Lumerical Solutions, Inc. www.lumerical.com/tcad-products/fdtd/.

(23) Attwood, D.; Sakdinawat, A. *X-Rays and Extreme Ultraviolet Radiation: Principles and Applications*, 2nd ed.; Cambridge University Press, 2017.

(24) Kipp, L.; Skibowski, M.; Johnson, R. L.; Berndt, R.; Adelung, R.; Harm, S.; Seemann, R. Sharper images by focusing soft X-rays with photon sieves. *Nature* **2001**, *414*, 184–188.

(25) Andersen, G. Large optical photon sieve. *Opt. Lett.* **2005**, *30*, 2976–2978.

(26) Gu, Y.; Zhang, L.; Yang, J. K. W.; Yeo, S. P.; Qiu, C.-W. Color generation via subwavelength plasmonic nanostructures. *Nanoscale* **2015**, *7*, 6409–19.

(27) Williams, C.; Montelongo, Y.; Tenorio-Pearl, J. O.; Cabrero-Vilatela, A.; Hofmann, S.; Milne, W. I.; Wilkinson, T. D. Engineered pixels using active plasmonic holograms with liquid crystals. *physica status solidi (RRL) Rapid Research Letters* **2015**, *9*, 125–129.

(28) Montelongo, Y.; Tenorio-Pearl, J. O.; Williams, C.; Zhang, S.; Milne, W. I.; Wilkinson, T. D. Plasmonic nanoparticle scattering for color holograms. *Proceedings of the National Academy of Sciences of the United States of America* **2014**, *111*, 12679–12683.

(29) Williams, C.; Rughoobur, G.; Flewitt, A. J.; Wilkinson, T. D. Nanostructured plasmonic metapixels. *Scientific Reports* **2017**, *7*, 7745.